

Flat bands and long range Coulomb interactions: conducting or insulating ?

Wolfgang Häusler

*Institut für Physik, Universität Augsburg, D-86135 Augsburg and
I. Institut für Theoretische Physik, Universität Hamburg, D-20355 Hamburg, Germany*

Dispersionless (flat) electronic bands are investigated regarding their conductance properties. Due to “caging” of carriers these bands are usually insulating at partial filling, at least on the non-interacting level. Considering the specific example of a \mathcal{T}_3 -lattice we study long-range Coulomb interactions. A non-trivial dependence of the conductivity on flat band filling is obtained, exhibiting an infinite number of zeros. Near these zeros, the conductivity rises linearly with carrier density. At densities half way in between adjacent conductivity-zeros, strongly enhanced conductivity is predicted, accompanying a solid-solid phase transition.

PACS numbers: 71.10.Fd, 71.10.-w, 73.20.Qt, 73.20.Jc, 73.90.+f

Recently, electronic flat bands in periodic lattices have received considerable attention [1], where single particle energies ε_k of at least one tight binding band stay non- or weakly dispersing, throughout the Brillouin zone. One focus of interest in two spatial dimensions, similar to Landau levels, is the effect of interactions which in the absence of kinetic energy always has to be treated non-perturbatively. Fractional Chern insulator (FCI) phases have been identified [2, 3], some of which exhibit Chern numbers larger than unity [4] and thereby generalize fractional quantum Hall states. Meanwhile, many lattices have been detected to host flat bands. Band flatness [5] arises due to localization by local quantum interferences, coined [6] as “caging” of carriers. As a result, the conductivity vanishes, at least on the noninteracting level. This accords with the vanishing Chern number of *strictly* flat single particle bands where $d\varepsilon_k/dk = 0$, throughout the Brillouin zone, as proven recently [7] for tight binding lattices.

On-site Hubbard interaction seems to delocalize vicinally caged carriers, which was considered as indication for nonzero conductivity [8]. However, short range interactions cannot impair the huge flat band degeneracy at low fillings [9]. Competing charge density wave phases have been studied [3]. Here, we investigate long range Coulomb interactions which at any filling will lift the flat band degeneracy. In quantum Hall systems, when kinetic energy is quenched, they cause Wigner crystallization at fillings $\nu < 1/5$ [10] (in graphene at $\nu < 0.28$ [11]) while without magnetic field crystallization appears when the Coulomb energy E_C exceeds the kinetic energy E_K by a sufficiently big factor [12], $E_C/E_K > 37$. The longitudinal conductivity

$$\sigma(\omega) = D \frac{1}{i\omega} \quad (1)$$

of clean systems at zero temperature diverges [13] and is then due to sliding of the hexagonal crystal as a whole [14]. Its Drude weight $D = e^2 n/m$ is determined by carrier density n and particle masses m , just as in the absence of interactions [15]; in this work we do not con-

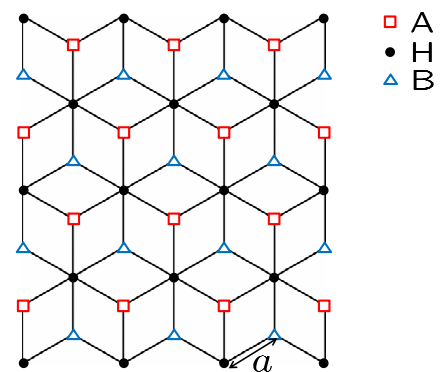


FIG. 1: Structure of the \mathcal{T}_3 -lattice: A (\square) and B (\triangle) sites are connected to only 3 nearest H (\bullet) sites, while conversely, H-sites are 6-fold coordinated. The structure implies equal numbers of lattice sites, $N_A = N_H = N_B$.

sider crystalline disorder. In flat bands, where no kinetic energy competes, we always expect a Wigner crystallized phase. Conductance properties, quantified again by the Drude weight D , cannot simply be proportional to m^{-1} since m is *a priori* meaningless to parameterize kinetic energy [5]. In this work we determine D of flat bands in the presence of (static) Coulomb interactions. Our main result is sketched in Fig. 2, below: D exhibits an infinite number of zeros at inverse band fillings, cf. Eq. (3). Near these zeros, the Drude weight rises linearly with slopes that we estimate. Right in the middle between adjacent insulating fillings phase transitions occur for which we expect strongly enhanced conductivities.

We analyze flat bands in two dimensions exemplarily for the \mathcal{T}_3 -lattice [6], which in literature also is called Sutherland- or dice-lattice, and which, in principle, can be realized on the basis of cold quantum gases [16, 17]. It consists of three different sublattices, (A,H,B), where A- and B-sites are not directly connected but only through H-sites, cf. Fig. 1.

Equal nearest neighbor hopping t across bonds of lengths a and zero hoppings between sites of larger distance gives rise to energy bands ε_k resembling much the band structure of graphene with two Dirac points at the corners of the hexagonal Brillouin zone and cone-like linearly dispersing bands in their vicinity. Additionally, at zero energy, there is a flat band extending throughout the Brillouin zone. In direct generalization to graphene, the long wave length Hamiltonian near one of the two inequivalent Dirac-points can be described in spinor form

$$H = v_F \mathbf{p} \cdot \mathbf{S} \quad (2)$$

when using spin-1 operators $\mathbf{S} = (S_x, S_y)$ [16, 18] (instead of spin-1/2 operators as for graphene) to describe pseudo-spins that encode now amplitudes on three sublattices (A,H,B), $v_F = 3ta/\sqrt{2}$ being the Fermi velocity. The carrier momentum \mathbf{p} in (2) formally serves as quantization axes for three pseudo-spin eigenstates of energies $\varepsilon_k^{(1,0,-1)} = (v_F|k|, 0, -v_F|k|)$. Here, we focus on the flat band $\varepsilon_k^{(0)} = 0$ with corresponding eigenstates $\psi_k^{(0)} = (-|k|e^{-i\varphi}, 0, |k|e^{i\varphi})/\mathcal{N}_k$ that manifest non-populated central H-sites ($|k|$ and $\varphi = \arctan k_y/k_x$ denote, respectively, modulus and direction of the carrier wave vector, and \mathcal{N}_k a normalization). A small spin-orbit term consisting of intrinsic and Rashba contributions [19] removes the Dirac point by opening a gap which perturbatively renormalizes to increasing values in the simultaneous presence of Coulomb interactions [19]; this isolates the flat band and, for small spin-orbit coupling strength, leaves $\psi_k^{(0)}$ essentially unaffected.

Linear combinations within the $(N/3)$ -fold degenerate space of flat band Bloch states ($N = N_A + N_H + N_B$ is the total number of lattice sites) allow to construct strictly localized states around any H-site, such that the entire amplitude resides just on one ring of six nearest A- and B-sites surrounding that given H-site, of equal magnitude but of alternating signs on A- and B-sites around the ring, and vanishes elsewhere. This describes spatial localization of ‘caged’ quantum states in a strictly periodic lattice [20]. At fillings $\nu = 3N_e^{(0)}/N \leq 1$ of the flat band only νN_H out of all rings are occupied, $N_e^{(0)}$ being the flat band carrier number.

Long range Coulomb interactions $\sim e^2/\kappa|\mathbf{r}-\mathbf{r}'|$ will lift the huge flat band degeneracy by favoring maximum distances between carriers, κ is the dielectric constant. On a continuous space the ground state would be a Wigner crystal [21] of lattice constant $b = \sqrt{3/\nu}a = \sqrt{2/\sqrt{3}n_e}$, where a is the \mathcal{T}_3 -lattice constant and $n_e = 2/\sqrt{3}b^2$ the flat band carrier density. Here, however, carriers cannot occupy arbitrary continuous positions but must reside at H-sites (more precisely, on rings surrounding H-sites) which constrains possible carrier positions to the hexagonal H-lattice of lattice constant $\sqrt{3}a$ with which b is in general incommensurate at arbitrary ν . Commensurabil-

$1/\nu_{n_1 n_2}$	n_1	n_2	$\theta_{n_1 n_2}$	$\Delta_{n_1 n_2}$
3	1	1	30.	1
4	2	0	0.	3
7	2	1	19.1066	2
9	3	0	0.	3
12	2	2	30.	1
13	3	1	13.8979	3
16	4	0	0.	3
19	3	2	23.4132	2
21	4	1	10.8934	4
25	5	0	0.	2
:				
1477	31	12	15.6886	6
1483	38	1	1.2886	5
1488	28	16	21.0517	1
1489	37	3	3.8606	3
1492	34	8	10.3327	5
1497	32	11	14.2536	4
1501	36	5	6.4171	15
1516	30	14	18.1432	3
1519	35	7	8.9483	2
1521	39	0	0.	3
:				

TABLE I: Some values of inverse commensurate fillings $\nu_{n_1 n_2}^{-1} = n_1^2 + n_2^2 + n_1 n_2$ satisfying (3) where (n_1, n_2) is one out of in general 12 pairs of associated integers. The angles $\theta_{n_1 n_2} = \arctan \sqrt{3}/(1 + 2n_1/n_2)$ in degrees (chosen here as $0 \leq \theta_{n_1 n_2} \leq 30^\circ$) describe how the corresponding Wigner crystal is oriented w.r.t. the \mathcal{T}_3 -lattice. Differences separating adjacent $\nu_{n_1 n_2}^{-1}$ are called $\Delta_{n_1 n_2}$.

ity between both hexagonal lattices necessitates

$$\frac{b}{\sqrt{3}a} = 1/\sqrt{\nu_{n_1 n_2}} \equiv \sqrt{n_1^2 + n_2^2 + n_1 n_2}, \quad n_1, n_2 \in \mathbb{Z} \quad (3)$$

for some pair of integers (n_1, n_2) . At fillings $\nu_{n_1 n_2}$ the Wigner crystal just ‘fits’ to \mathcal{T}_3 -lattice sites. Tab. 1 lists some typical examples for $\nu_{n_1 n_2}^{-1} = n_1^2 + n_2^2 + n_1 n_2$ satisfying (3). At commensurate fillings $\nu_{n_1 n_2}$ the conductivity vanishes, as demonstrated below. We remark that seemingly random distances $\sim \Delta_{n_1 n_2}$ separate adjacent commensurate fillings, with bigger $\Delta_{n_1 n_2}$ occurring rarer. This resembles somewhat to prime numbers though, at the moment, we are unable to estimate the asymptotic decay for the occurrence of large $\Delta_{n_1 n_2}$ as a function of the magnitude of $\Delta_{n_1 n_2}$.

Wigner crystallization spontaneously breaks translational and rotational symmetries so that the ensuing crystal at $\nu = \nu_{n_1 n_2}$ will be oriented at angle $0 \leq \theta_{n_1 n_2} \leq \pi/6$ w.r.t. the underlying \mathcal{T}_3 -lattice, where $\tan \theta_{n_1 n_2} = \sqrt{3}/(1 + 2n_1/n_2) = \tan(\pi/3 - \theta_{n_2 n_1})$. Accounting additionally for the trivial hexagonal symmetry, $\theta_{n_1 n_2} \rightarrow \theta_{n_1 n_2} + n\pi/3$ for $n = 1, \dots, 5$, there are altogether 12 pairs of integers (n_1, n_2) characterizing commensurate Wigner lattices at same flat band carrier density [22]. As a result, crystals of adjacent commensu-

rate densities will be more or less randomly oriented, cf. Tab. 1.

How does the ground state look like at fillings $\nu = \nu_{n_1 n_2} + \delta\nu$ for $|\delta\nu| \ll \nu^2$ slightly deviating from commensurate values $\nu_{n_1 n_2}$? To accommodate additional ($\delta\nu > 0$) or missing ($\delta\nu < 0$) carriers the system has basically two options: *i*) develop two domains out of two adjacent commensurate fillings each, or *ii*) accommodate, as $\nu_{n_1 n_2}$ -Wigner crystal, $\delta\nu N_H$ additional ‘electrons’ at interstitial places or leave $\delta\nu N_H$ vacant Wigner sites as ‘holes’, depending on the sign of $\delta\nu$. Simple energetic estimate supports the more homogeneous ground state *ii*) near commensurate fillings since domains would suffer energetically from additional charging, dipolar, and surface contributions.

For conductance properties we analyze the current density

$$\mathbf{j} = v_F \mathbf{S}, \quad (4)$$

which for \mathcal{T}_3 resembles the relativistic expression for the operator \mathbf{j} of graphene [13, 23]. In \mathcal{T}_3 , spin matrices

$$S_x = \frac{1}{\sqrt{2}} \begin{pmatrix} 0 & 1 & 0 \\ 1 & 0 & 1 \\ 0 & 1 & 0 \end{pmatrix}, \quad S_y = \frac{1}{\sqrt{2}} \begin{pmatrix} 0 & -i & 0 \\ i & 0 & -i \\ 0 & i & 0 \end{pmatrix}, \quad (5)$$

substitute Pauli-matrices. We see that matrix elements $\langle \psi_k^{(0)} | \mathbf{j} | \psi_{k'}^{(0)} \rangle$ vanish identically inside the flat band, as a result of vanishing H-occupancy. In consequence, the system is insulating since the conductivity is proportional to squares of these matrix elements, in accordance with the above caging argument. Finite conductivity necessitates finite amplitudes on H-sites which, in turn, requires to destroy the destructive quantum interference responsible for caging on hexagonal rings surrounding H-sites, for example by derogating the precise balance in the occupation probabilities of A- and B-sites through asymmetric electrostatic forces induced by proximate charges.

For commensurate crystals the entire environs of each Wigner site are hexagonally symmetric for any (n_1, n_2) . While electrostatic forces created by vicinal Wigner sites will act on all 6 A- and B-sites encircling a given Wigner site, enhancing e.g. their on-site potential energies, and the magnitudes of respective hoppings t_A and t_B to nearest H-sites, no *difference* between A and B arises, $t_A = t_B$, leaving thus caging intact. Therefore, at fillings $\nu = \nu_{n_1 n_2}$ the flat band stays insulating in the presence of long range Coulomb interactions.

The situation can change at fillings $\nu = \nu_{n_1 n_2} + \delta\nu$. In the following we focus on low flat band fillings, $\nu \ll 1$, such that $b \gg a$, cf. (3). While both types of ‘dopants’, electrons and holes, may distort the crystal in their vicinity [?] [however, at most by discrete displacements, constrained to H-sites — we do not consider elastic distortion of the underlying \mathcal{T}_3 -lattice here, having in mind for example optical lattices] to relax local electrostatic

strain this effect will have minor impact on the conductivity, and is therefore neglected in the following. Energetically, interstitials prefer positions right in the middle of Wigner triangles, at distances $b/\sqrt{3}$ to nearest Wigner-sites, while vacancies are just unoccupied Wigner-sites.

Generally, electrons as well as each of the six Wigner sites next to holes experience non-hexagonally symmetric environs which may mobilize them. Crucial for emerging A-B-imbalance are electrostatic forces acting *differently* on A- and B-sublattices. Nearest electrostatic centers located on perpendicular bisectors of the A- and B-sites still do *not* achieve such an imbalance, albeit now $t_{A,B}$ ’s may vary in magnitude as we go around the 6 sites of an occupied ring while mirror symmetry remains preserved. This kind of symmetry occurs when $\theta_{n_1 n_2} = \pi/6$ for $\delta\nu > 0$ (electrons) and $\theta_{n_1 n_2} = 0, \pi/3$ for $\delta\nu < 0$ (holes). As a result, near fillings $\nu_{n_1 n_2}$ where $\theta_{n_1 n_2} = \{0 \text{ or } \pi/3\}$ we expect vanishing conductance yet over a finite interval $\nu = \nu_{n_1 n_2} \pm |\delta\nu|$.

At all other fillings $\nu = \nu_{n_1 n_2} + \delta\nu$ (with $\delta\nu \neq 0$) destructive quantum interference and local topological localization of dopants is destroyed, H-sites acquire non-zero amplitude, and a finite delocalizing kinetic energy arises (which then has to compete with the Coulomb energy as in the ordinary Wigner transition). In principle, this allows dopants to spread across the entire \mathcal{T}_3 -lattice, resulting in finite conductivity. To quantify the potential *difference* between A- and B-sites of a hexagon cage due to an asymmetric Coulomb field let us consider some charge at distance $d \gg a$ from the ring center which induces amplitude

$$u_H \sim \frac{e^2}{\kappa v_F} \frac{a^2}{d^2} \left(\left(\frac{3}{2} \right)^{3/2} - \frac{3}{\sqrt{2}} \right) \left| \begin{cases} \cos 3\theta_{n_1 n_2} \\ \sin 3\theta_{n_1 n_2} \end{cases} \right| \quad (6)$$

for $\begin{cases} \text{electrons} \\ \text{holes} \end{cases}$

at the ring center and at the same time on H-sites outside the considered ring. It depends on the angle $\theta_{n_1 n_2}$ of the Wigner crystal orientation; $d = b/\sqrt{3}$ or $d = b$ for interstitials (electrons) or vacancies (holes), respectively. The dimensionless prefactor $e^2/\kappa v_F$ in (6) may be regarded as ‘effective fine structure constant’, parameterizing the interaction strength [24]. Within a continuum theory, employed from now on at $\nu \ll 1$ for transport properties, the non-zero amplitude (6) on H-sites effectively results in kinetic energy of dopants, associated with a mass

$$m_{\text{eff}} = 1/(v_F a |u_H|), \quad (7)$$

which promotes tunneling through Coulomb barriers to nearest interstitial or vacancy places at distances $b/\sqrt{3}$ or b , respectively.

As a result, dopants effectively experience a periodic Coulomb potential landscape created by caged Wigner charges. Ignoring correlations between dopants and using

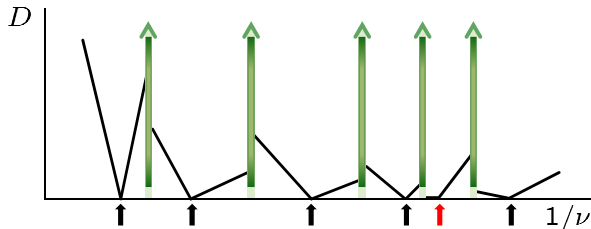


FIG. 2: Drude weight D versus inverse flat band filling $1/\nu$, schematically. When $\nu = \nu_{n_1 n_2}$, cf. eq. (3), $D = 0$. Near these zeros (arrows), D rises linearly $\propto |\delta\nu|$ (unless $\theta_{n_1 n_2} = \pi/6 + \mathbb{Z} \pi/3$ or $\theta_{n_1 n_2} = \mathbb{Z} \pi/3$ when D stays constantly zero to the left or right of $\nu_{n_1 n_2}$, respectively (red arrow)). In the middle between two adjacent zeros of D , (green shaded rectangular areas), the system exhibits a first order phase transition: there the Drude weight is expected to rise considerably.

path integral methods, the dopants matrix element

$$t_{e/h} = \Delta e^{-S_0} \quad (8)$$

for hopping between adjacent minima can be estimated within a dilute instanton gas approximation [25]. Eq. (8) results from summing over all possible series of independent instanton actions

$$S_0 = 2\sqrt{\frac{e^2 m_{\text{eff}}}{\kappa}} \int_{-d/2}^{d/2} dx (x^2 + 3d^2/4)^{-1/4} = C_1 \sqrt{\frac{e^2 m_{\text{eff}}}{\kappa}} \sqrt{d} \quad (9)$$

for motions in the inverted Coulomb potential $-V(x) = -\frac{2e^2}{\kappa} / \sqrt{x^2 + 3d^2/4}$ by distances d during imaginary times. We assumed that dominant parts of the Coulomb barrier are created by two charges at distances $\sqrt{3}d/2$ ‘off the way’ which holds true for electron as well as for hole tunneling, $C_1 \approx 2.096$ is a numerical factor which can be expressed analytically in terms of hypergeometric functions.

Estimates for the ratio Δ of fluctuation determinants in (8) are possible when considering the periodic Coulomb potential $V_0(1 - \cos 2\pi x/d)$ along the tunnel trajectory with $V_0 = \frac{2e^2}{\kappa d}(\frac{2}{\sqrt{3}} - 1)$; then [26]

$$\Delta = \frac{16V_0}{(m_{\text{eff}}V_0)^{1/4} \sqrt{d/2}}. \quad (10)$$

Now we are in the position to estimate the Drude weight $D = e^2 n_D / m_{e/h}$ in eq. (1). Here, $n_D = (|\delta\nu|/\nu)n_e = 2|\delta\nu|/3^{3/2}a^2$ is the density and the band mass for itinerant electron/hole type dopants takes values $m_{e/h} = 1/(2t_{e/h}d^2)$, respectively, cf. (8) [note that $m_{e/h}$ differs from the kinetic energy mass m_{eff}]. Combining Eqs. (6–10), our result for the Drude weight becomes

$$D = \frac{e^2 n_D}{m_{e/h}} = C_2 \frac{e^2}{\kappa a} \gamma \nu^{-1/8} e^{-S_0} \left\{ \begin{array}{l} \cos 3\theta_{n_1 n_2} \\ \sin 3\theta_{n_1 n_2} \end{array} \right\}^{1/4} |\delta\nu|, \quad (11)$$

where

$$S_0 = C_3 (\nu \gamma)^{-3/2} \left| \begin{array}{l} \cos 3\theta_{n_1 n_2} \\ \sin 3\theta_{n_1 n_2} \end{array} \right|^{-1/2}$$

for $\begin{cases} \text{electrons} \\ \text{holes} \end{cases}$, $\gamma = \begin{cases} 3 \\ 1 \end{cases}$,

and $C_2 = 5.276$ and $C_3 = 20.43$ being again constants that can be expressed analytically.

Qualitatively, this result (11) is sketched in Fig. 2 versus $1/\nu$. Starting from zeros at commensurate fillings $\nu_{n_1 n_2}$ the Drude weight rises linearly with small $|\delta\nu| = |\nu - \nu_{n_1 n_2}|$. Slopes tend to decrease with decreasing filling ν , however, depending on the orientations $\theta_{n_1 n_2}$, they may differ strongly from one zero to the next one. In symmetric cases, $\theta_{n_1 n_2} = \pi/6 + \mathbb{Z} \pi/3$ (electrons) or $\theta_{n_1 n_2} = \mathbb{Z} \pi/3$ (holes) the Drude weight stays constantly zero over a finite range of fillings on one side of $1/\nu_{n_1 n_2}$, cf. red arrow in Fig. 2. When the density of electron type dopants from a lower density $\nu_{n_1 n_2}$ commensurate Wigner crystal equals the density of hole type dopants from the next higher density $\nu_{n'_1 n'_2}$ Wigner crystal, i.e. right in the middle between two adjacent commensurate fillings $\nu_{n_1 n_2}$ and $\nu_{n'_1 n'_2}$ (green shaded areas in Fig. 2), according to Landau’s rule, a first order solid to solid phase transition takes place. While sweeping carrier density the system has to transform *all* Wigner sites (n_1, n_2) at crystal orientation $\theta_{n_1 n_2}$ into the next set of Wigner sites (n'_1, n'_2) at crystal orientation $\theta_{n'_1 n'_2}$. Therefore, at the phase transition caging should be destroyed entirely and we expect a drastic increase of the Drude weight during a transport measurement, up to values of the order $e^2 n_e / m_{\text{eff}}$ which exceeds the estimate (11) by a large factor $\sim (\nu/|\delta\nu|)e^{S_0}$.

In conclusion, we have studied the Drude weight of flat band insulators at zero temperature in the presence of long range Coulomb interactions. A non-trivial function of density is found, exhibiting infinitely many zeros at commensurate fillings, given by eq. (3). Near those fillings the Drude weight varies linearly with filling. Sweeping the filling under transport conditions, first order phase transitions of the electron crystal should cause considerably enhanced Drude weights right in the middle between adjacent commensurate fillings.

I am indebted to Reinhold Egger for many inspiring discussions and acknowledge gratefully sharing aspects of related research with Dario Bercioux and with Daniel Urban. I thank Peter Talkner for a valuable feed back on the manuscript, Peter Hänggi for providing fruitful working conditions, and the State of Bavaria for still supporting fundamental research.

[1] E.J. Bergholtz, Z. Liu, Int. J. Mod. Phys. B **27**, 1330017 (2013); S.A. Parameswaran, R. Roy, S.L. Sondhi,

- Comptes Rendus Physique **14**, 816 (2013), and references therein.
- [2] E. Tang, J.-W. Mei, X.-G. Wen, Phys. Rev. Lett. **106**, 236802 (2011); K. Sun, Z. Gu, H. Katsura, S. Das Sarma, Phys. Rev. Lett. **106**, 236803 (2011); T. Neupert, L. Santos, C. Chamon, C. Mudry, Phys. Rev. Lett. **106**, 236804 (2011); A.M. Läuchli, Z. Liu, E.J. Bergholtz, R. Moessner, Phys. Rev. Lett. **111**, 126802 (2013).
- [3] S. Kourtis, J.W.F. Venderbos, M. Daghofer, Phys. Rev. B **86**, 235118 (2012).
- [4] F. Wang, Y. Ran, Phys. Rev. B **84**, 241103(R) (2011); A. Sterdyniak, C. Repellin, B.A. Bernevig, N. Regnault, Phys. Rev. B **87**, 205137 (2013); Z. Liu, E.J. Bergholtz, H. Fan, A.M. Läuchli, Phys. Rev. Lett. **109**, 186805 (2012); S. Kourtis, T. Neupert, C. Chamon, C. Mudry, Phys. Rev. Lett. **112**, 126806 (2014).
- [5] Band flatness cannot be regarded as the limit of band mass m going to infinity, e.g. in a dispersion $\varepsilon_k \propto k^2/2m$ which would yield finite conductance in this limit due to the simultaneously increasing density of states $\propto dk(\varepsilon)/d\varepsilon$ that cancels the effect of decreasing velocity $\propto d\varepsilon_k/dk$.
- [6] J. Vidal, R. Mosseri, B. Douçot, Phys. Rev. Lett. **81**, 5888 (1998).
- [7] L. Chen, T. Mazaheri, A. Seidel, X. Tang, J. Phys. A: Math. Theor. **47**, 152001 (2014).
- [8] J. Vidal, B. Douçot, R. Mosseri, P. Butaud, Phys. Rev. Lett. **85**, 3906 (2000); J. Vidal, P. Butaud, B. Douçot, R. Mosseri, Phys. Rev. B **64**, 155306 (2001); Z. Gulácsi, A. Kampf, D. Vollhardt, Phys. Rev. Lett. **99**, 026404 (2007).
- [9] C. Wu, S. Das Sarma, Phys. Rev. B **77**, 235107 (2008); S. Takayoshi, H. Katsura, N. Watanabe, H. Aoki, Phys. Rev. A **88**, 063613 (2013).
- [10] See, for example, H.W. Jiang, R.L. Willett, H.L. Stormer, D.C. Tsui, L.N. Pfeiffer, K.W. West, Phys. Rev. Lett. **65**, 633 (1990).
- [11] C.-H. Zhang, Y.N. Joglekar, Phys. Rev. B **75**, 245414 (2007); O. Poplavskyy, M.O. Goerbig, C. Morais Smith, Phys. Rev. B **80**, 195414 (2009).
- [12] B. Tanatar, D.M. Ceperley, Phys. Rev. B **39**, 5005 (1989).
- [13] M. Vigh, L. Oroszlány, S. Vajna, P. San-Jose, G. Dávid, J. Cserti, B. Dóra, Phys. Rev. B **88**, 161413(R) (2013).
- [14] R. Chitra, T. Giamarchi, Eur. Phys. J. B **44**, 455 (2005); pinning of Wigner crystals by disorder is beyond the scope of the present work.
- [15] W. Kohn, Phys. Rev. **123**, 1242 (1961).
- [16] D. Bercioux, D.F. Urban, H. Grabert, W. Häusler, Phys. Rev. A **80**, 063603 (2009).
- [17] For non time reversal invariant generalizations cf. B. Dóra, I.F. Herbut, R. Moessner, arXiv:1402.6532, (2014).
- [18] D. Green, L. Santos, C. Chamon, Phys. Rev. B **82**, 075104 (2010); B. Dóra, J. Kailasvuori, R. Moessner, Phys. Rev. B **84**, 195422 (2011).
- [19] C.L. Kane, E.J. Mele, Phys. Rev. Lett. **95**, 226801 (2005).
- [20] B. Sutherland, Phys. Rev. B **34**, 5208 (1986).
- [21] G. Meissner, H. Namaizawa, M. Voss, Phys. Rev. B **13**, 1370 (1976); L. Bonsall, A.A. Maradudin, Phys. Rev. B **15**, 1959 (1977).
- [22] Unless $|n_1| = |n_2|$ or $n_i = 0$ when only 6 different pairs (n_1, n_2) exist.
- [23] D.F. Urban, D. Bercioux, M. Wimmer, W. Häusler, Phys. Rev. B **84**, 115136 (2011).
- [24] In suspended graphene, for example, its magnitude is of order $2.2/\kappa$, I. Sodemann, M. M. Fogler, Phys. Rev. B **86**, 115408 (2012).
- [25] S. Coleman in *The Whys of Subnuclear Physics*, Springer Subnuclear Series **15**, ed. by A. Zichichi (1979).
- [26] J. Zinn-Justin, Nucl. Phys. B **192**, 125 (1981); Z. Ambroziński, Acta Physica Polonica B, **44**, 1261 (2013).